Article

Cell

Compartmentalization of a Bistable Switch Enables Memory to Cross a Feedback-Driven Transition

Graphical Abstract

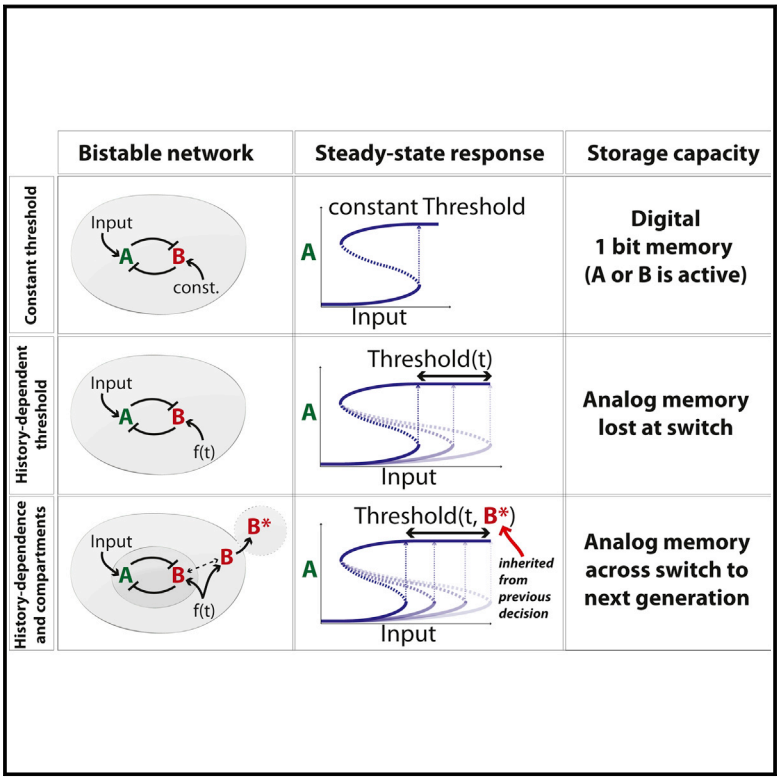

Authors

Andreas Doncic, Oguzhan Atay, ..., Mart Loog, Jan M. Skotheim

Correspondence

skotheim@stanford.edu

In Brief

The spatial organization of the G1/S switch enables the intergenerational transmission of memory of pheromone exposure in budding yeast.

Highlights

- Yeast decide to enter the cell cycle based on the history of pheromone exposure
- Compartmentalization enables transmission of memory from mother to daughter
- Intergenerational memory of pheromone exposure is stored as cytoplasmic Far1
- Anchoring of cytoplasmic Far1 by Cdc24 is required for intergenerational memory

Doncic et al., 2015, Cell *160*, 1182–1195
March 12, 2015
http://dx.doi.org/10.1016/j.cell.2015.02.032

CellPress

Cell

Article

Compartmentalization of a Bistable Switch Enables Memory to Cross a Feedback-Driven Transition

Andreas Doncic,[1] Oguzhan Atay,[1] Ervin Valk,[2] Alicia Grande,[3] Alan Bush,[3] Gustavo Vasen,[3] Alejandro Colman-Lerner,[3] Mart Loog,[2] and Jan M. Skotheim[1,*]

[1]Department of Biology, Stanford University, Stanford, CA 94305, USA

[2]Institute of Technology, University of Tartu, 50411, Estonia

[3]IFIBYNE-UBA-CONICET and Departamento de Fisiología, Biología Molecular y Celular, Facultad de Ciencias Exactas y Naturales, Universidad de Buenos Aires, Buenos Aires C1428EHA, Argentina

*Correspondence: skotheim@stanford.edu

http://dx.doi.org/10.1016/j.cell.2015.02.032

SUMMARY

Cells make accurate decisions in the face of molecular noise and environmental fluctuations by relying not only on present pathway activity, but also on their memory of past signaling dynamics. Once a decision is made, cellular transitions are often rapid and switch-like due to positive feedback loops in the regulatory network. While positive feedback loops are good at promoting switch-like transitions, they are not expected to retain information to inform subsequent decisions. However, this expectation is based on our current understanding of network motifs that accounts for temporal, but not spatial, dynamics. Here, we show how spatial organization of the feedback-driven yeast G1/S switch enables the transmission of memory of past pheromone exposure across this transition. We expect this to be one of many examples where the exquisite spatial organization of the eukaryotic cell enables previously well-characterized network motifs to perform new and unexpected signal processing functions.

INTRODUCTION

Cellular signaling pathways are used to transmit information about the extra- and intra-cellular environment. Specific outputs from such signaling pathways are then used by decision-making networks to determine cellular response. Currently, signaling pathways are most often described as static schematics based on a combination of genetic dependencies and biochemical interactions. While a good first step, such a characterization can neither describe nor predict the pathway dynamics that determine cellular response to time-dependent input signals (Behar et al., 2008; Yosef and Regev, 2011). Indeed, outputs of the regulatory networks controlling proliferation and apoptosis depend on the history of dynamic input signals, not only on current levels (Doncic and Skotheim, 2013; Lee et al., 2012; Purvis et al., 2012). This strongly suggests that the ability to retain information from prior states is a key determinant informing cellular decision making.

Signaling dynamics play important roles in many networks regulating switch-like transitions between distinct states. The switch-like nature of transitions often arises from positive feedback loops that quickly increase the activity of key regulatory proteins when triggered by input signals above a specific threshold. Networks containing positive feedback loops frequently give rise to bistability, i.e., for a range of input signals, the output will be one of two possible values depending on the history of the input signal. However, this is a very simple form of history dependence as all possible time-dependent input signals get mapped onto only two possible outputs, i.e., history dependence is collapsed onto only a single bit of information. This implies that while positive feedback loops may be good at promoting switch-like transitions, they appear unable to retain more than rudimentary information about signaling pathway history. It is therefore improbable that a positive-feedback-driven switch can be used to transmit information to inform future cellular decisions. However, this conclusion is based on the current framework for analyzing network motifs such as feedback-loops or feed-forward interactions (Alon, 2007), which accounts for temporal but not spatial dynamics. Thus, while it is well-known that spatial organization plays an important role in signal transduction, we do not currently know how or if the eukaryotic cell's spatial organization can affect existing motif functions or give rise to entirely new motif functions (Howell et al., 2012; Kholodenko et al., 2010; Santos et al., 2012).

To better understand how spatial organization might affect cellular signal processing, we decided to examine the cell-cycle control network responsible for the decision to divide in budding yeast. In yeast, the decision to commit to cell division takes place in late G1, prior to DNA replication at a point called *Start* (Hartwell et al., 1974). Multiple internal and external signals are integrated to determine when a cell passes *Start*, beyond which cells no longer respond to mating pheromone (α-factor). *Start* is a switch-like, irreversible transition that corresponds to the activation of a positive feedback loop of cyclin-dependent kinase (Cdk1) activity (Doncic et al., 2011). Specifically, Cln3-Cdk partially inactivates Whi5, a transcriptional inhibitor of the expression of the G1 cyclins *CLN1* and *CLN2*. The expression of Cln1 and Cln2 complete inactivation of Whi5 by forming a positive feedback loop (Costanzo et al., 2004; de Bruin et al., 2004; Skotheim et al., 2008).

Prior to *Start*, cells can be arrested by pheromone-dependent activation of the mitogen activated protein kinase (MAPK) mating pathway (Chen and Thorner, 2007). Upon pheromone exposure, the MAPK Fus3 phosphorylates and activates the Cdk inhibitor Far1, which inhibits the G1 cyclins essential for progression through *Start* (Chang and Herskowitz, 1990; Gartner et al., 1998; Jeoung et al., 1998; Peter et al., 1993; Pope et al., 2014; Tyers and Futcher, 1993). Conversely, post-*Start*, the G1 cyclins inhibit the mating pathway by targeting the upstream scaffold protein Ste5 as well as Far1 (Garrenton et al., 2009; Henchoz et al., 1997; Peter and Herskowitz, 1994; Strickfaden et al., 2007; Tyers and Futcher, 1993) (Figure S1A). Thus, progression through *Start* drives an increase in cyclin expression that results in Far1 degradation, whereas pre-*Start* exposure to pheromone leads to Far1 activation, G1 cyclin inhibition, and G1 arrest (Doncic et al., 2011; McKinney et al., 1993; Pope et al., 2014). In other words, the regulatory network underlying *Start* is bistable, where a well-defined commitment point separates stable low- and high-Cdk activity states, and only the low-Cdk activity state can be inhibited by MAPK signaling (Doncic et al., 2011).

Although this characterization of *Start* is accurate for a step input of high pheromone concentration, cells exposed to low or intermediate pheromone concentrations do not arrest permanently, but rather delay progression through G1 (Hao et al., 2008; Malleshaiah et al., 2010; Moore, 1984). This suggests a more complex decision making machinery that balances the benefits of successful mating with the costs of staying arrested and both failing to mate and proliferate. Thus, while the *Start* network remains bistable, its output changes from a digital response to arrest or not, to an analog computation determining how long to arrest before reentering the cell division cycle. We previously showed that in this analog computation, yeast cells decide to reenter the cell cycle based on their history of exposure to pheromone during an arrest, not just the current pathway activity (Doncic and Skotheim, 2013). Time-dependent pheromone signals are processed by the MAPK pathway using a coherent feed-forward motif in which the MAPK Fus3 activates Far1 both by direct phosphorylation and by increasing its expression via the Ste12 transcription factor (Chang and Herskowitz, 1990; Errede and Ammerer, 1989; Gartner et al., 1998) (Figure S1A; red arrows). This architecture allows a robust yet rapidly reversible cellular state. Far1 accumulates to provide a memory so that cells exposed to pheromone for longer durations have more Far1 rendering them more reluctant to reenter the cell cycle. In addition, fast dephosphorylation allow Far1 to be rapidly inactivated so that cells can rapidly reenter the cell cycle if the MAPK signal plummets (Doncic and Skotheim, 2013).

Although the accumulation of Far1 provides a mechanism to remember the history of pheromone exposure during a single arrest, it does not suggest a mechanism to transmit this information to subsequent generations after cell-cycle reentry. This is because the mutual inhibition of Cdk and Far1 activity underlying the bistable *Start* switch is expected to target all Far1 for degradation once the cell cycle has been reentered. Similarly, the sharp switch at mitotic exit also employs ultra-sensitive protein degradation (Yang and Ferrell, 2013). Protein degradation may be useful to sharpen switches and reset regulatory circuits, but comes at the cost of losing cellular memory. Thus, while bistable regulatory networks are excellent at generating all-or-none transitions, they limit the amount of information that can be propagated across these transitions.

Here, we show how compartmentalization of the bistable G1 control network allows cellular memory to traverse the *Start* switch. Far1 is split into nuclear and cytoplasmic pools that combat distinct sets of cyclin-Cdk complexes allowing these two compartments of the Far1-Cdk switch to have distinct dynamics. Upon reentering the cell cycle from pheromone arrest, nuclear Far1 is rapidly degraded, while cytoplasmic Far1 is degraded much more slowly so that a substantial pool remains at the beginning of the next division cycle. We show that this inherited pool contributes to cell-cycle arrest in the daughter cells so that the mother cells are able to transmit their memory of pheromone exposure to the next generation. This intergenerational memory depends on the anchoring of Far1 to cytoplasmic Cdc24, a regulator of cell polarization. Thus, we demonstrate how compartmentalization of a bistable regulatory circuit enables an entirely new function to be performed by this well-characterized signaling motif. More broadly, our results argue that spatial organization can greatly enhance the function of regulatory motifs and is therefore just as integral to pathway function as network topology and chemical kinetics.

RESULTS

Nuclear Far1 and Nuclear Cln2 Function in Cell-Cycle Commitment

To determine if and how signal information could be propagated across a bistable switch, we examined the network regulating *Start*, the point of commitment to cell division in budding yeast (Figure 1A). Since cyclin-Cdk complexes phosphorylate Far1 to target it for degradation, we expected that Far1 would be rapidly degraded upon progression through *Start*.

To examine the localization and dynamics of Far1, we used a Far1-Venus fusion protein expressed from the endogenous locus (Figure 1B). This *FAR1-Venus* strain exhibited the same arrest kinetics as an unlabeled WT strain, and we will subsequently refer to *FAR1-Venus* strains as WT (Doncic and Skotheim, 2013). Unless specified otherwise, all strains are in a background lacking the Bar1 protease that cleaves mating pheromone (for strain and plasmid lists see Table S1 and Table S2). Cells were arrested in high pheromone (240 nM α-factor) and released into pheromone-free medium using a previously described microfluidics-based assay (Doncic et al., 2011). Consistent with previous results (McKinney et al., 1993), Far1 was synthesized during mating arrest and mostly degraded post-*Start* after release into pheromone-free medium. However, the examination of Far1-Venus using time-lapse microscopy revealed a striking spatial dichotomy in Far1 degradation kinetics. The nuclear pool of Far1 is rapidly degraded in less than 10 min (approximately 7 min after *Start*), which is defined as when 50% of Whi5 has been exported from the nucleus (Doncic et al., 2011). Nuclear Far1 is degraded at approximately the same time as the Cdk-B-type cyclin inhibitor Sic1, which we previously measured as occurring ~8 min after *Start* (see Figures S1B and S1C for Far1 degradation

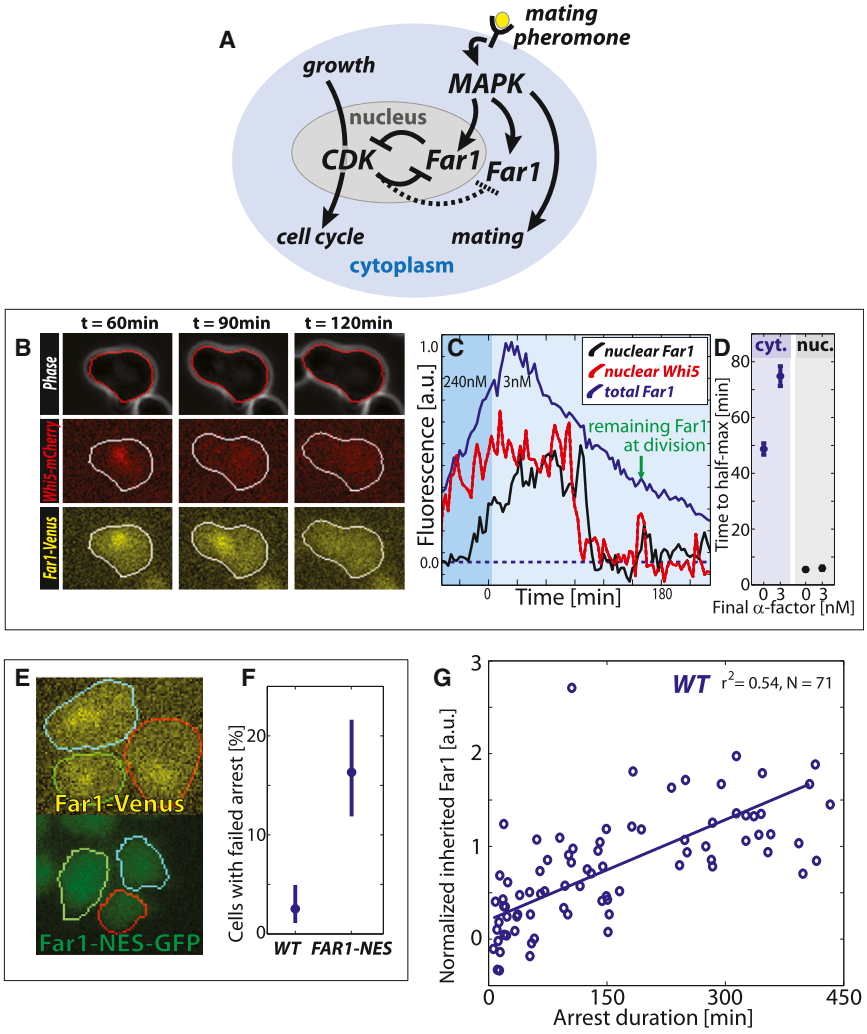

Figure 1. Cytoplasmic Far1 Is Inherited to Provide Intergenerational Memory across the *Start* Switch

(A) Schematic of the double-negative feedback (equivalent to positive feedback) network that regulates the switch between cell-cycle progression and pheromone arrest.

(B) Example images of segmented phase, Whi5-mCherry (red) and Far1-Venus (yellow) channels for cells reentering the cell cycle. Whi5-mCherry is nuclear in arrested cells.

(C) Example time series of nuclear Whi5-mCherry, and nuclear and cytoplasmic Far1-Venus that corresponds to the cell shown in (B). Nuclear Far1 is much more rapidly degraded than cytoplasmic Far1.

(D) Time from peak to half-maximum for cytoplasmic and nuclear Far1 in cells arrested in 240 nM and released into either 3 or 0 nM pheromone.

(E) Example *FAR1-Venus* and *FAR1-NES-GFP* cells arrested in 240 nM for 2 hr show that the nuclear localization is diminished in the *FAR1-NES-GFP* cells.

(F) A larger fraction of pre-*Start FAR1-NES* cells fails to arrest when abruptly exposed to 240 nM pheromone, where *Start* is defined as removal of 50% of nuclear Whi5-mCherry.

(G) Inherited Far1 in daughter cells is correlated with arrest duration.

Error bars in (D) denote SEM, while error bars in (F) denote 95% confidence intervals from 10,000 bootstrap iterations.

timing and (Doncic et al., 2011) for Sic1 degradation timing). This implies that Far1 degradation is likely coincident with the appearance of B-type cyclin activity in the nucleus. However, the cytoplasmic pool lingered and reached half-maximum ~50 min after *Start* (Figures 1C and 1D). This observed difference in Far1 degradation kinetics may be due to the nuclear F-box protein Cdc4 that mediates Far1 degradation (Blondel et al., 2000). This demonstrates that there are two separate pools of Far1 protein being degraded on very different time scales.

The rapid degradation of nuclear Far1 upon progression through *Start* suggests that it is primarily this nuclear pool that contributes to the commitment decision in response to exposure to pheromone (Blondel et al., 1999; Blondel et al., 2000). To test this, we added a nuclear export sequence to the endogenous *FAR1* allele (*FAR1-NES*), which greatly reduced the nuclear pool without affecting expression levels (Figures 1E and S1D). We then examined the cellular response to an abrupt increase in pheromone in the framework we previously developed to examine *Start* (Doncic et al., 2011). When exposed to a step-increase of pheromone, pre-*Start FAR1-NES* cells were over six times more likely than WT cells to fail to arrest despite not having traversed the Whi5-threshold (16% *FAR1-NES* versus 2.5% WT, Figure 1F). In addition, we found that nuclear, but not cytoplasmic Cln2 participated in *Start* (Figures S1E–S1I). Taken together, these results support a role for nuclear Far1 in *Start*.

Cytoplasmic Far1 Provides Intergenerational Memory of Pheromone Exposure

Even though nuclear Far1 was important for *Start*, most Far1 in arrested cells (~90%) is cytoplasmic and is not degraded rapidly upon cell-cycle reentry (Figures S2A–S2E). In fact, cytoplasmic Far1 is so slowly degraded after cell-cycle reentry that appreciable quantities are passed on to subsequent generations (Figures 1C and S2F). This is surprising because once cells reenter the cell cycle, these mother cells are desensitized to that level of pheromone and divide repeatedly without delay (Figure S2G) (Caudron and Barral, 2013; Doncic and Skotheim, 2013; Moore, 1984). To examine the role of inherited Far1 in daughter cells, we briefly arrested cells at high pheromone concentration (240 nM) before releasing the cells into an intermediate pheromone concentration (3 nM). The time to reach half-maximum Far1 post-*Start* in 3 nM pheromone was ~5 min in the nuclear pool and ~75 min in the cytoplasmic pool (Figure 1D). Thus, the time to reach cytoplasmic half-maximum post-*Start* is

increased relative to cells reentering in pheromone-free medium. Consequently, daughter cells entering the cell cycle in 3 nM pheromone inherited an increased amount of Far1 compared to daughter cells entering the cell cycle in pheromone-free medium (Figure S2H). This finding, that cells cycling in higher pheromone concentrations pass increasing amounts of Far1 on to their daughter cells, led us to hypothesize that inheritance of cytoplasmic Far1 is the molecular basis of an *intergenerational memory* of pheromone exposure.

To test the *intergenerational memory* hypothesis, we measured both the amount of inherited Far1 and subsequent G1 duration for daughter cells cycling in 3 nM, an intermediate mating pheromone concentration (see Experimental Procedures and Figure S2I). The more Far1 a daughter cell inherited, the longer it delayed progression through G1, supporting the hypothesis that mother cells transmit information about pheromone exposure to their daughters through cytoplasmic Far1 (Figure 1G). We also examined if differential inheritance of MAPK pathway scaffold Ste5, which affects pheromone signaling in a dosage-dependent manner (Thomson et al., 2011), could affect arrest duration, but found no effect (Figure S2J and S2K).

Compartmentalization Is Supported by a Fixed Fraction of Cytoplasmic Far1

The rapid degradation of the nuclear, but not cytoplasmic pool of Far1, requires a slow exchange between these two pools. Indeed, it would be impossible to maintain Far1 post-*Start* if Far1 were exchanged rapidly between the two pools as the half-life of nuclear Far1 is ~5 min. To investigate this requirement, we photobleached the nucleus of *FAR1-Venus* cells and measured the recovery of nuclear fluorescence (Figure 2A). Pre-*Start* cells were identified by examining the localization of Whi5-mKO fusion proteins expressed from the endogenous locus. After photobleaching, a significant recovery of the nuclear fraction on the 10 s timescale was seen. However, the nuclear to cytoplasmic fluorescence ratio did not recover to its initial level and reached a plateau prior to 30 s (Figures 2B–2D). Note that there is little new protein synthesis or degradation over the time frame of the experiment so that nearly all the recovery is due to protein translocation. The incomplete recovery of the nuclear-to-cytoplasmic ratio of Far1-*Venus* indicates that there is a pool of Far1 molecules that does not shuttle between the nucleus and the cytoplasm. As a control, we examined recovery of the yellow fluorescent protein YFP expressed from an *ACT1* promoter. The YFP nuclear-to-cytoplasmic ratio completely recovered after bleaching, which is consistent with rapid and unencumbered shuttling between nucleus and cytoplasm (Figure 2D). Taken together, we here identify both a rapidly shuttling and a fixed pool of Far1, which supports our model for how compartmentalization is used to generate intergenerational memory.

To transmit intergenerational memory, there should be a fixed cytoplasmic pool of Far1. While a single FRAP experiment indicates the presence of a fixed Far1 pool, it does not identify its location. To determine if there is fixed Far1 in the cytoplasm, we photobleached the nucleus four times sequentially and measured depletion of cytoplasmic Far1-Venus or YFP (Figures 2E and 2F). In the case of YFP, there is no fixed pool, so that the nuclear-to-cytoplasmic ratio recovers after each photobleaching event. Thus, each bleaching of the nucleus bleaches a constant fraction of the total protein. This leads to a linear relationship between the logarithm of the fluorescence and the number of photobleaching events (see Supplemental Information). A fixed cytoplasmic pool would result in a deviation from this linear fit. To test for a fixed cytoplasmic pool, we fit the normalized logarithm of the cytoplasmic fluorescence to a quadratic equation for each cell (Figure 2G). We find positive quadratic coefficients for Far1-Venus fits indicating the presence of a pool of Far1 that is fixed in the cytoplasm (Figure 2H).

Pheromone Exposure Is Remembered across the Entire Cell Cycle

To better understand intergenerational memory, we sought to investigate the mechanisms responsible for the increased time to half-maximum concentration of Far1 in 3 nM relative to 0 nM pheromone (Figure 1D). Such an increase could arise due to either increased Far1 synthesis or decreased Far1 degradation, or both. To test for regulated protein degradation, we expressed a *FAR1-Venus* fluorescent fusion protein from a galactose-inducible *GAL1* promoter. We inactivated Far1 synthesis by switching the carbon source from galactose to glucose and measured Far1 half-life post-*Start* (Figure 3A). Far1 stability post-*Start* is only weakly sensitive to pheromone concentration, which suggests that continued synthesis is more likely than increased protein stability to underlie increased inheritance of cytoplasmic Far1 at intermediate pheromone concentrations (Figures 3B and S4A). To test this possibility, we used single molecule fluorescence in situ hybridization (smFISH) (Raj et al., 2008), to measure the amount of *FAR1* mRNA transcripts (Figure 3C). Indeed, *FAR1* transcription was higher in 3 nM compared to 0 nM for cells with small and medium sized buds, corresponding to S and G2 cells respectively (Figures 3D). For large budded cells, likely about to divide, the number of *FAR1* transcripts was similarly high for both conditions, consistent with previous work showing that *FAR1* and other Ste12 transcription factor targets are transcribed at the M/G1 transition, even at 0 nM pheromone (Doncic and Skotheim, 2013; McKinney et al., 1993; Oehlen et al., 1996).

To test if the increased Far1 transcription in intermediate pheromone concentrations results from MAPK pathway activity, we examined *STE5-YFP* cells expressing the mating pathway scaffold protein Ste5 fused to a yellow fluorescent protein (Yu et al., 2008). Ste5 localizes to the site of polarized growth when the mating pathway is active (Pryciak and Huntress, 1998; Strickfaden et al., 2007). *STE5-YFP* cells were arrested in 3 nM pheromone and tracked through a cell cycle. The cell perimeter was segmented, linearized, and plotted on a kymograph to visualize the location and intensity of Ste5-YFP on the cell membrane (Figures 3E and 3F). As expected, we observed a transition from a low to a high level of Ste5-YFP at the site of polarized growth upon pheromone arrest (Figure 3G). Upon reentering the cell cycle, Ste5-YFP only partially dissociates from the membrane suggesting that the MAPK pathway remains active through the cell cycle at intermediate pheromone concentrations ($p < 0.05$ for all comparisons, Figure 3H). We

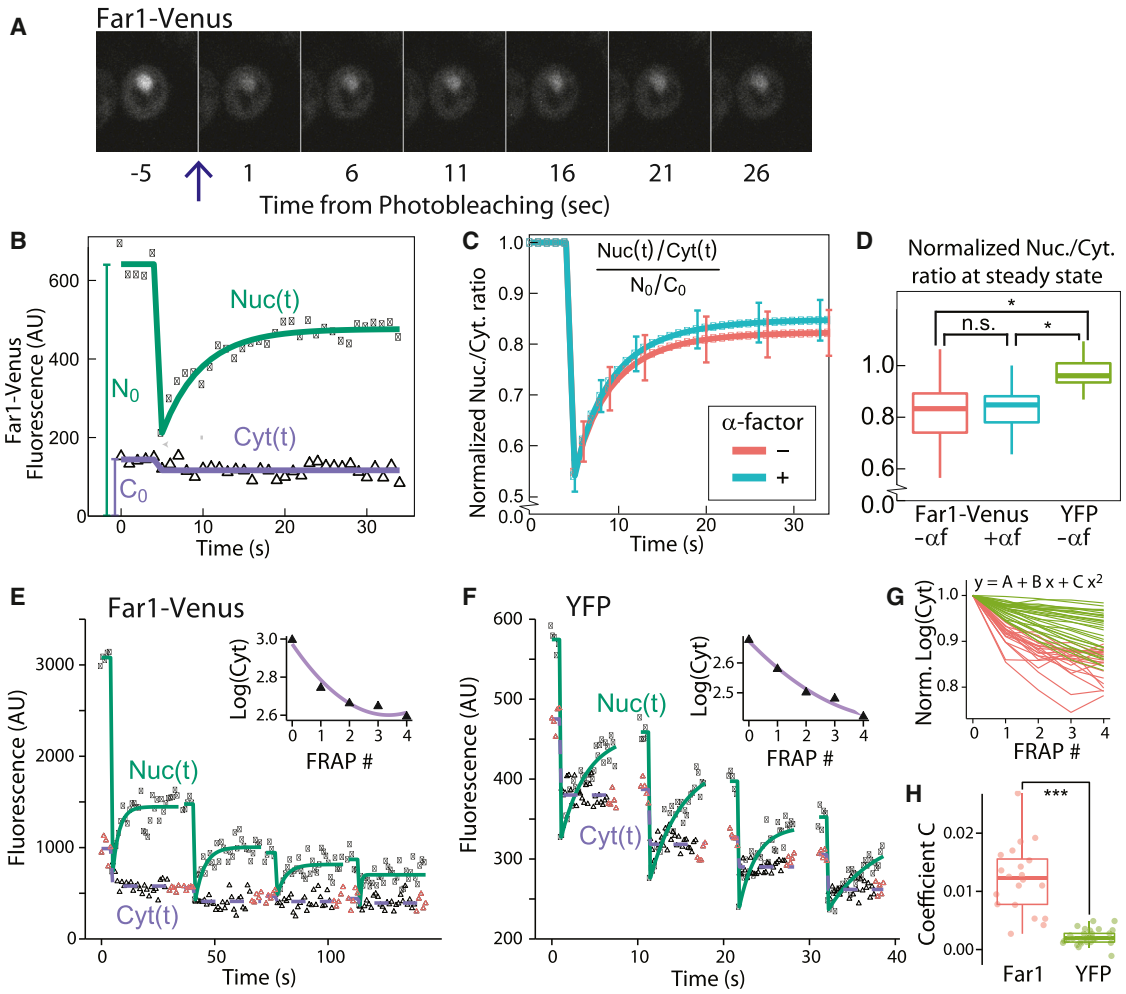

Figure 2. A Pool of Far1 Is Fixed in the Cytoplasm

(A) Fluorescence images from a typical time course, where the nuclear Far1-Venus was photobleached at t = 0.

(B) Data and model fit for nuclear, *Nuc(t)*, and cytoplasmic, *Cyt(t)*, Far1. N_0 and C_0 denote the initial nuclear and cytoplasmic fluorescence.

(C) Mean nuclear-to-cytoplasmic ratio of Far1-Venus normalized to its initial value, N_0/C_0. Bars denote the 95% confidence interval of the mean. We examined pre-*Start* G1 cells either not exposed to α-factor (red) or exposed to 500 nM α-factor (blue).

(D) Distribution of the estimated steady-state value of the normalized Nuc/Cyt ratio after photobleaching. Cells expressing Far1-Venus (blue/red) do not recover the initial nuclear-to-cytoplasmic ratio, while cells expressing the fluorescent protein YFP from an integrated ACT1 promoter (green) recover the initial ratio (see also Figure S3).

(E and F) Nuclear and cytoplasmic fluorescence from Far1-Venus or YFP following four sequential photobleaching events. Inset shows logarithm base 10 of the mean steady-state cytoplasmic fluorescence following the indicated photobleaching event and the associated quadratic fit. Red triangles denote data points used for steady-state estimates.

(G) Single cell data for cytoplasmic steady-state fluorescence after normalization to its value prior to the first bleaching event for Far1-Venus (red) and YFP (green).

(H) Distribution of coefficients C for the quadratic term of the quadratic fit. C = 0 indicates a linear relationship between the logarithm of the cytoplasmic fluorescence and the number of photobleaching events, which corresponds to the case with no fixed cytoplasmic pool. C > 0 indicates the presence of a fixed cytoplasmic pool (see Supplemental Information).

*denotes $p < 0.05$, ***denotes $p < 0.001$, n.s denotes $p > 0.05$. Tukey boxplots in (D) and (H) indicate median, upper, and lower quartiles. Whiskers extend to the most extreme point within 1.5× the interquartile range.

also tested if the MAPK Fus3 is active in S/G2/M cells (post-*Start*) exposed to pheromone as implied by the above results. Fus3 activity correlates with increased nuclear localization and phosphorylation (Blackwell et al., 2003). We therefore measured Fus3 activity using time lapse microscopy and western blot with a phosphospecific antibody (Nagiec and Dohlman, 2012). Consistent with MAPK (Fus3) activity being responsive to pheromone concentration in cycling cells, Fus3-GFP nuclear localization quickly decreased in cells in the S/G2/M phases of the cell cycle that experienced a drop in extracellular pheromone concentration (Figures S4B–S4D; $p < 10^{-4}$). Similarly, exposure of cells in the S/G2/M phases of the cell cycle to pheromone increased the amount of phosphorylated Fus3 (Figures 3I–3K). Moreover, we immunoprecipitated Fus3 from S/G2/M cells

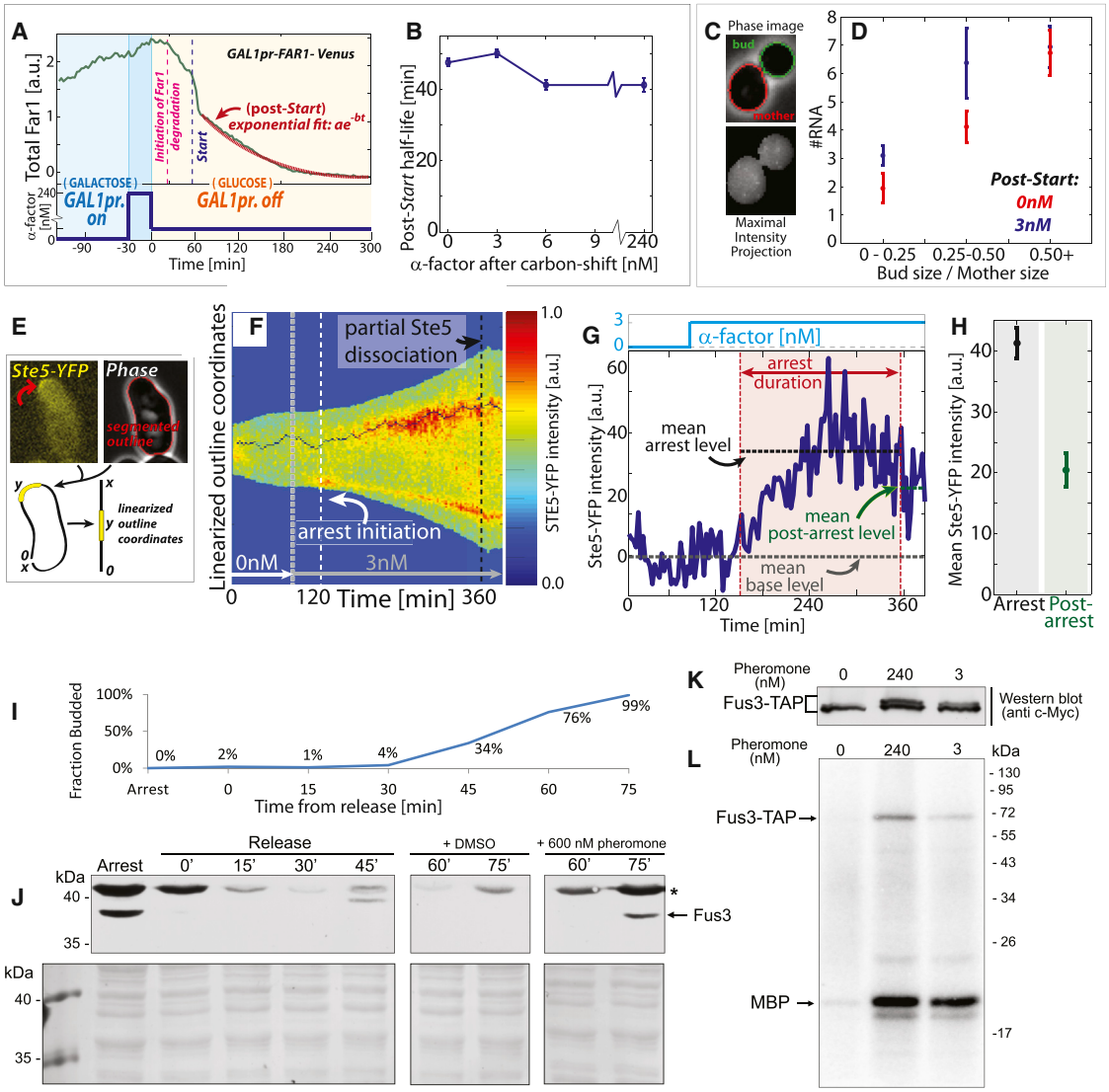

Figure 3. Pheromone Exposure Post-*Start* Is Remembered

(A) Experiment schematic for measuring stability of Far1 protein post-*Start*.

(B) Post-*Start* half-life measured after release from pheromone arrest in 240 nM to 0, 3, 6 and 240 nM.

(C) Example of segmented phase image of mother cell body (red) and bud (green) and their corresponding smFISH maximal intensity projections. Each dot represents a single *FAR1* mRNA.

(D) Mean number of *FAR1* mRNA in cells having small, medium, and large buds.

(E) Example segmented phase and Ste5-YFP fluorescence images for a cell arrested in 3 nM α-factor. Ste5-YFP localizes to the site of polarized growth.

(F) Kymograph of example cell in (E). The amount of Ste5 at the site of polarized growth, whose location was determined using the Viterbi algorithm (Forney, 1973).

(G) Ste5-YFP trace of example cell shown in (F) indicating levels before, after, and during arrest.

(H) Mean Ste5-YFP intensity at the site of polarized growth for pre- and post-*Start* cells in 3 nM. Membrane fluorescence prior to pheromone addition was background subtracted. $p < 0.05$ for all comparisons.

(I–L) Cells were arrested in G1 using pheromone and released synchronously through the cell cycle. Fifty minutes after release, after commitment to division, cells were re-exposed to pheromone (see methods). (I) Bud index. (J) Top: western blot time course with a phospho-specific antibody indicates presence of phosphorylated Fus3 in S/G2/M cells exposed to pheromone; (bottom) Ponceau stained blots are provided as loading controls. (K and L) Fus3-TAP was immunoprecipitated at the 75 min time point, when nearly all cells were in S/G2/M, for cells in 0, 3 or 240 nM pheromone. (K) Western blot for this IP indicating increasing Fus3 phosphoshifts in 3 and 240 nM pheromone. (L) Fus3 activity on MBP was measured in an in vitro kinase assay using radiolabeling.

Error bars in (B), (D) and (H) denote SEM.

exposed to 0, 3 and 240 nM pheromone. IP-Fus3 phosphorylated a substrate (MBP) at a rate increasing with pheromone concentration (Figure 3L).

Taken together, our data support a model in which cells cycling in intermediate pheromone concentrations have increased cytoplasmic Far1 levels due to a partially active

MAPK pathway post-*Start*. Thus, while it is clear that cell-cycle progression inhibits pheromone signaling (Garrenton et al., 2009; Strickfaden et al., 2007; Torres et al., 2011), this inhibition is not complete at intermediate pheromone concentrations. Our data thus shows that intergenerational memory is composed of Far1 accumulated from the entire previous cell division cycle. In other words, cells remember pheromone exposure post-*Start* as well as pre-*Start* from the previous cell division cycle.

Decreasing Cytoplasmic Far1 Reduces Intergenerational Memory

Our results so far support the model in which an *intergenerational* memory of pheromone exposure is transmitted to newborn daughter cells via stable cytoplasmic Far1. If true, we predict that reducing inherited Far1 by genetic manipulation would result in shorter arrest durations in daughter cells. It was previously shown that deletion of the S-phase cyclins *CLB5* and *CLB6,* but not the G1 cyclins *CLN1* and *CLN2*, resulted in longer arrest durations in 3 nM pheromone (Doncic and Skotheim, 2013) and that ectopic expression of Clb5 downregulates Far1 (Oehlen et al., 1998). In addition, the S-phase cyclins are nuclear, where Far1 is rapidly degraded (Blondel et al., 2000; Shirayama et al., 1999). We therefore constructed a *CLB5-NES* strain by adding a nuclear export sequence to *CLB5* (Figure 4A). In this strain, the time to half-maximum post-*Start* of cytoplasmic Far1 in 3 nM pheromone was ~45 min, a significant reduction from the ~75 min half-maximum of wild-type cells (Figures 4B and 4C and S5A,B; $p < 0.01$).

In G1, Far1 will be stable because Clb5 is targeted for degradation by the APC/C following mitosis (Shirayama et al., 1999). Thus, while *CLB5-NES* cells have less cytoplasmic Far1, we expect the smaller amount of inherited Far1 to be just as functional in restraining passage through *Start* as in WT cells. That is, given the same amount of inherited Far1, *CLB5-NES* cells would arrest for similar durations as WT cells. Consistent with these predictions, *CLB5-NES* cells inherited less Far1 and remained arrested for shorter durations relative to WT (Figures 4D, 4E, and S5C). Also as predicted, the relationship between inherited Far1 and arrest duration was statistically similar to WT (Figures 4F and 4G; $p > 0.1$). These data support the interpretation that the *CLB5-NES* allele affects intergenerational memory through a reduction in inherited cytoplasmic Far1 prior to cytokinesis.

Reducing Inherited Far1 Lowers Mating Efficiency

While our results indicate an intergenerational memory of pheromone exposure from mother to daughter cells, it remains unclear if this intergenerational memory plays a role under other physiological conditions. To test this possibility, we performed a quantitative mating assay using WT and *CLB5-NES* strains. WT cells are able to mate more frequently than *CLB5-NES* cells (Figure 4H, $p < 0.05$). To test that this decrease in mating frequency was not due to a polarization defect we verified that *CLB5-NES* cells polarize similarly to WT cells in presence of a pheromone gradient (Figure S5D). These experiments are consistent with a role for intergenerational memory in physiological conditions.

Far1 Binding to Cdc24 Is Required for Intergenerational Memory

Our results so far identify an intergenerational memory arising from the stability of cytoplasmic Far1. This implies that a non-shuttling cytoplasmic pool of Far1 is inherited to transmit intergenerational memory. Consistent with this model, Far1 has binding partners in the cytoplasm, which we hypothesize serve to anchor Far1. A prime candidate for anchoring is Cdc24, a GTP exchange factor (GEF) regulating cell polarization. Far1 binding to Cdc24 is necessary for pheromone gradient sensing, but not for cell-cycle arrest (Nern and Arkowitz, 1999; Valtz et al., 1995) (Figure 5A). Moreover, Cdc24 is nuclear in G1, but is partially exported to the cytoplasm and plasma membrane during mating arrest in a Far1-dependent manner (Nern and Arkowitz, 2000; Shimada et al., 2000).

To test whether the interaction between Cdc24 and Far1 is required for intergenerational memory, we created strains with the endogenous *FAR1* allele replaced by either *FAR1-D1A* or *FAR1-H7* mutant alleles that express Far1 proteins whose interaction with Cdc24 is greatly reduced (Nern and Arkowitz, 2000; Valtz et al., 1995). As previously reported, both strains arrest in pheromone. However, we identified a slight arrest deficiency and 6 nM pheromone was required to arrest cells for similar durations as WT cells in 3 nM ($p > 0.05$). We therefore used 6 nM for the analysis of *FAR1-D1A* and *FAR1-H7* strains. Consistent with Cdc24 anchoring Far1 in the cytoplasm during arrest, the nuclear fraction of Far1 was increased in *FAR1-D1A* and *FAR1-H7* cells compared to WT cells ($p < 10^{-3}$; Figures 5B, S6A, and S6B). Since nuclear Far1 is rapidly degraded in the cell cycle (Figure 1D), we expected that reduction of cytoplasmic anchoring results in a more rapidly degraded Far1 protein. Indeed, Far1 proteins with reduced Cdc24 interactions reach half-maximum concentration more rapidly following cell-cycle entry (Figures 5C, S6C, and S6D). Finally, we examined the relationship between intergenerational memory and inherited Far1 in *FAR1-D1A* and *FAR1-H7* cells. Consistent with the requirement of a cytoplasmic anchor, and the model that Cdc24 fills this role, post-*Start* Far1 was less stable, less Far1 was inherited, and the intergenerational memory was abolished or greatly reduced in cells expressing Far1 proteins with reduced ability to bind Cdc24 (Figures 5D–5F and S6E–S6G).

To further test the Cdc24 anchoring model, we sought to examine *bni1Δ* cells that are unable to export Cdc24 from the nucleus to the shmoo tip during pheromone arrest (Qi and Elion, 2005). Bni1 is a formin that regulates the polarization of actin cables during mating arrest and is required for cell polarization (Evangelista et al., 1997). We found that *bni1Δ* cells arrested as round cells for significant periods of time in G1 when exposed to 6 nM pheromone (Figure S6H). Under these conditions, *bni1Δ* cells contained a higher fraction of nuclear Far1, and degraded Far1 more rapidly upon cell-cycle entry compared to WT cells (Figures 5B, 5C, S6B, and S6C). Finally, *bni1Δ* cells exhibited no intergenerational memory (Figure 5G). That the localization of Cdc24 outside the nucleus was required for intergenerational memory further supports the role of cytoplasmic Cdc24 as a Far1 anchor.

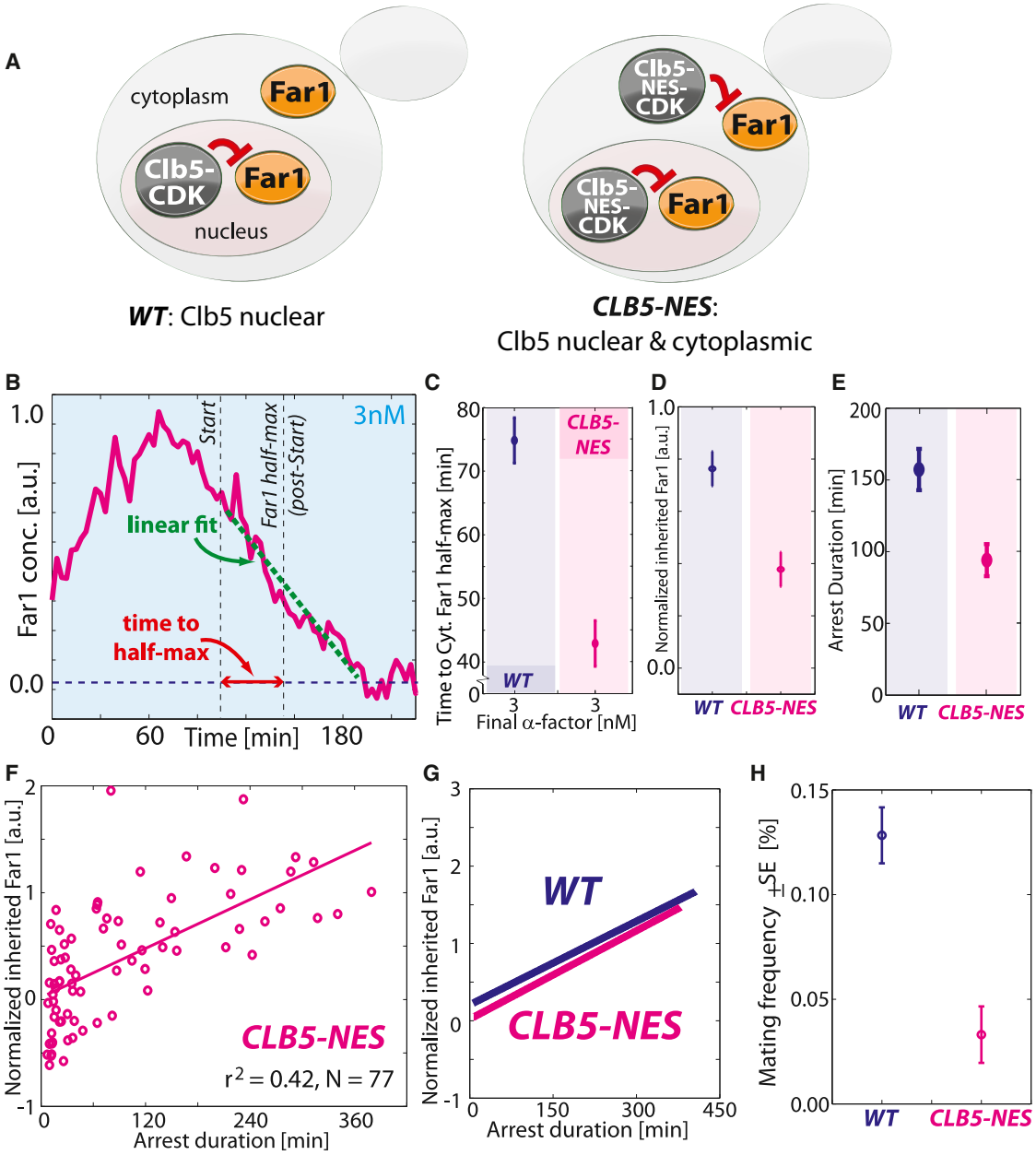

Figure 4. Reduction of Cytoplasmic Far1 Decreases Intergenerational Memory

(A) Clb5 targets Far1 for degradation and is predominantly nuclear in WT cells. Adding a nuclear exclusion sequence (NES) to *CLB5* translocates a fraction to the cytoplasm to target cytoplasmic Far1.

(B) Example time series of Far1 concentration in a *CLB5-NES* cell used to calculate the time to half-maximum post-*Start* for cytoplasmic Far1.

(C) Mean time to cytoplasmic Far1 half-maximum post-*Start* for WT and *CLB5-NES* cells first arrested in 240 nM and then released into 3 nM α-factor.

(D) *CLB5-NES* cells inherit less Far1 than WT and (E) arrest significantly shorter duration ($p < 10^{-5}$).

(F and G) The relationship between the amount of inherited Far1 and the duration of the subsequent arrest is statistically indistinguishable for *CLB5-NES* and WT cells ($p > 0.05$).

(H) WT and *CLB5-NES* cells exhibit significantly different mating frequencies ($p < 0.05$).

Error bars denote SEM of cells in (C–E) or of replica experiments in (H).

Far1 Stability Pre- and Post-*Start* Is Required for Intra- and Inter-Generational Memory Respectively

The intergenerational memory that we describe here is in addition to the *intragenerational memory* of pheromone exposure encoded in Far1 that we previously described (Doncic and Skotheim, 2013). Intragenerational memory allows cells to remember their history of exposure to pheromone during an arrest via the accumulation of Far1. Since Clb5 is targeted for

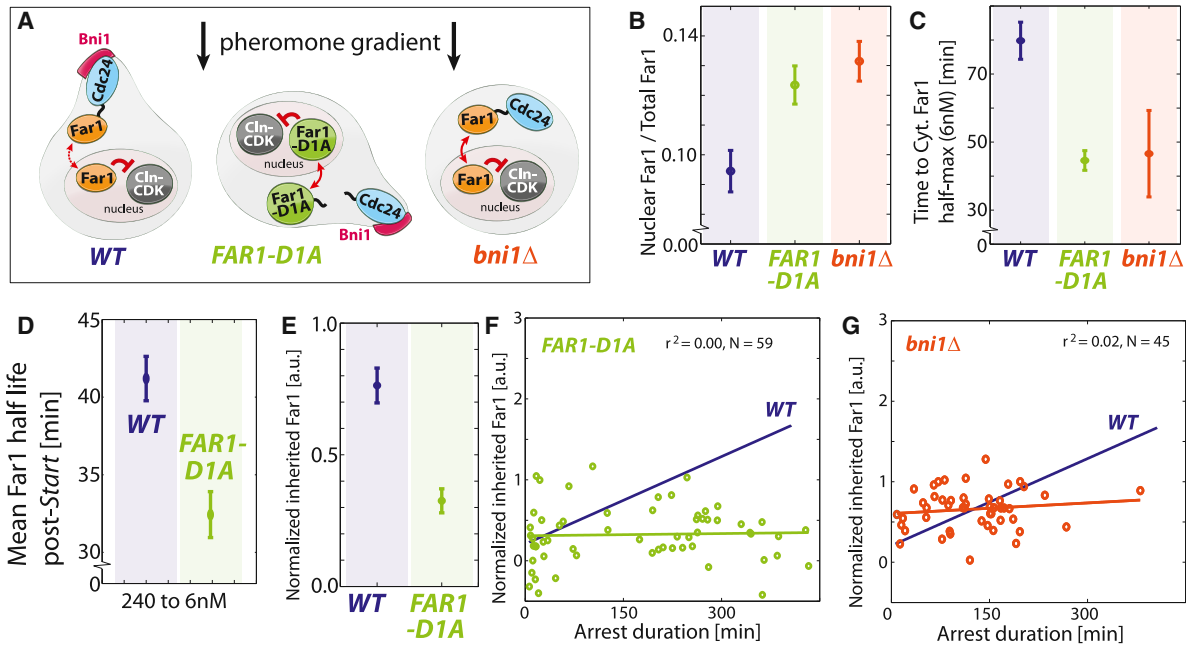

Figure 5. Far1 Binding to Cytoplasmic Cdc24 Is Required for Intergenerational Memory

(A) Schematic of the role of Cdc24 with respect to Far1.

(B) Fraction of nuclear Far1 in arrested cells.

(C) Time to half-maximum Far1 after cell-cycle reentry in 6 nM pheromone.

(D) The post-*Start* stability of Far1-D1A measured as described in Figure 3A.

(E) Inherited Far1 in *FAR1-D1A* cells compared to *WT* ($p < 10^{-4}$).

(F and G) No intergenerational memory was observed for *FAR1-D1A* and *bni1Δ* cells.

Error bars in (B–E) denote SEM.

degradation in mitosis, and is therefore not active during pheromone arrest, we do not expect cytoplasmic Clb5 to affect intragenerational memory. To test this prediction, we examined cell-cycle progression in cells exposed to different histories of mating pheromone during G1. Cells were either exposed to a brief pulse of high pheromone followed by an intermediate pheromone concentration or just to the intermediate pheromone concentration (Figure 6A). As predicted, both WT and *CLB5-NES* cells experiencing the high pheromone pulse greatly extended arrest duration indicating that while *CLB5-NES* cells have reduced intergenerational memory, their intragenerational memory remains firmly intact (Figures 6B and S7A–S7D). Furthermore, these experiments demonstrate how intergenerational memory is distinct from intragenerational memory and affected by different mutations.

Just as intergenerational memory depends on the stability of Far1 throughout the cell cycle, intragenerational memory should depend on the stability of Far1 during arrest. To destabilize Far1 during pheromone arrest, we generated a *FAR1* allele with the 92nd residue mutated from Leucine to Proline (*FAR1-L92P*). This mutation is predicted to generate an additional Cdk consensus phosphorylation site to enhance the degradation of Far1 (E.V. and M.L., unpublished data; Figure S7E). To control for the potentially pleiotropic effects of the L92P mutation, we also generated a *FAR1-PEST* allele, where an otherwise WT *FAR1* allele was fused to the C terminus of *CLN2,* which destabilizes this cyclin (Lanker et al., 1996). To determine the stability of Far1-L92P and Far1-PEST proteins during arrest, we fused them to GFP and expressed them from a *GAL1* promoter. Consistent with these mutations reducing protein stability, the pre-*Start* half-lives of Far1-L92P and Far1-PEST were reduced to ~50 and ~20 min respectively compared to over 130 min for WT Far1 (Figures 6C and 6D).

To test the dependence of intragenerational memory on Far1 stability, we next constructed a strain containing a single copy of *FAR1-L92P* expressed from its endogenous locus. However, *FAR1-L92P* cells failed to arrest even at high pheromone concentrations. We therefore constructed a strain containing 10-12 copies of *FAR1-L92P* that arrested as WT cells (72 ± 4 min for WT and 61 ± 7 min for *FAR1-L92P* in 2.7 nM pheromone, p = 0.17). To verify that the activity of Far1 remains unaltered in the *FAR1-L92P* strain we also showed that the ability of *12xFAR1-L92P* cells to polarize toward pheromone gradients was similar to WT cells (Figure S7F). Consistent with memory depending on Far1 stability, *12xFAR1-L92P* cells exhibited little if any intragenerational memory despite retaining the ability to arrest at this pheromone concentration (Figures 6B and S7A–S7C). In addition, *12xFAR1-L92P* cells also exhibit no intergenerational memory, most likely because this phenomenon also depends on Far1 stability (Figure 6E). Similarly, the destabilized *FAR1-PEST* strain greatly reduced both intra- and inter-generational memory (Figures 6B, 6F, S7A, and S7G). Taken together, these experiments

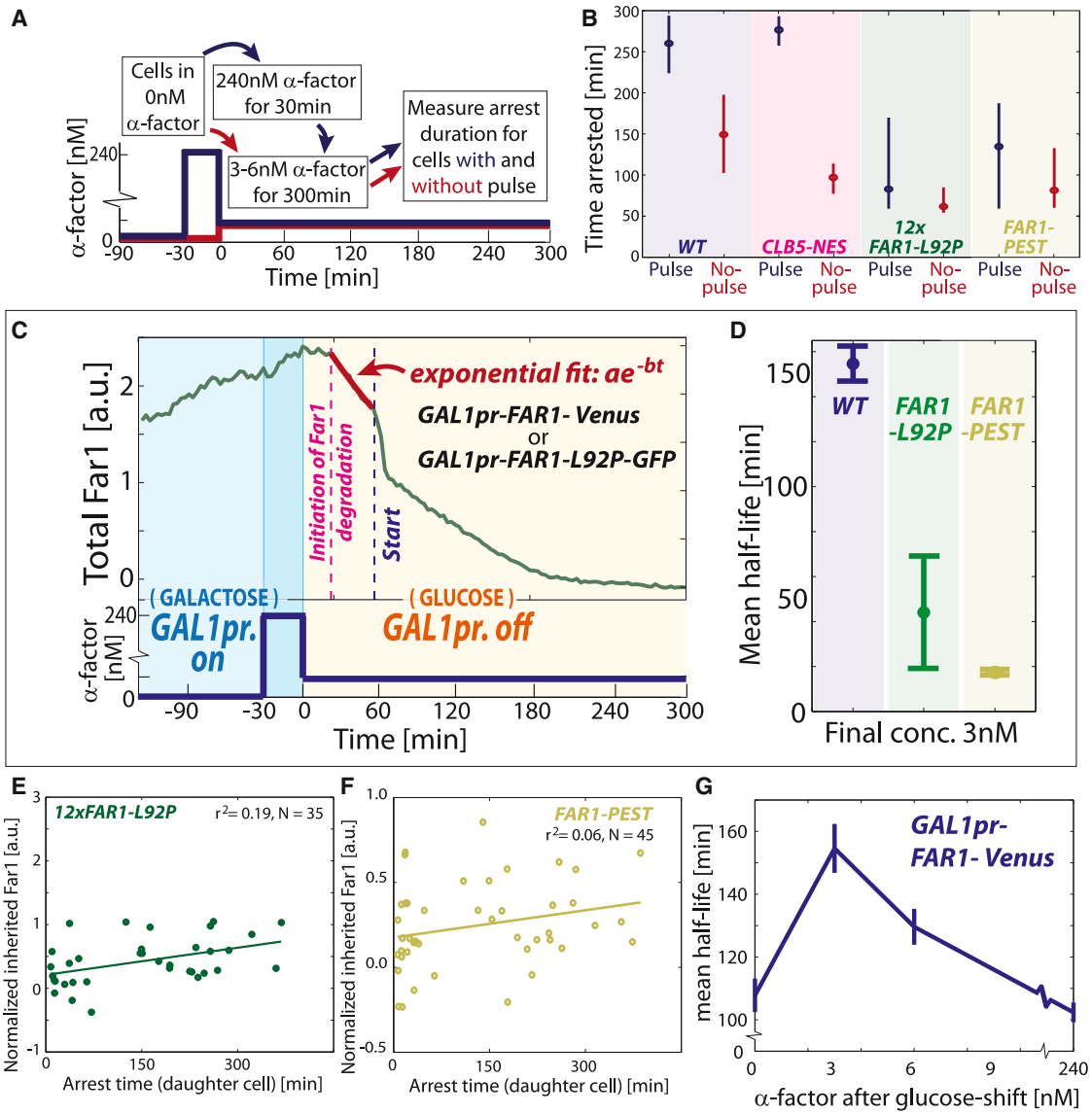

Figure 6. Protein Stability Is Required for Intra- and Inter-Generational Memory

(A) Experimental schematic for *intragenerational* memory experiment.

(B) WT and *CLB5-NES* cells have intragenerational memory, where the decision to reenter the cell cycle is based on the history of pheromone exposure during the arrest, while *12xFAR1-L92P* and *FAR1-PEST* cells do not. Medians plotted with 95% confidence intervals computed using 10,000 bootstrap iterations. Note that about half of both the *CLB5-NES* and WT cells exposed to a pulse of high mating pheromone are arrested for the duration of the experiment (Figure S7B). We therefore do not compare arrest durations for WT and *CLB5-NES* cells exposed to a pheromone pulse.

(C) Conditional expression of *FAR1* from a *GAL1* promoter is used to measure half-life pre-*Start* in a series of pheromone concentrations.

(D) Far1 half-life pre-*Start* in WT, *FAR1-L92P*, and *FAR1-PEST* cells in 3 nM α-factor.

(E and F) *12xFAR1-L92P* and *FAR1-PEST* cells lack intergenerational memory as their arrest duration is independent of the amount of inherited Far1.

(G) Conditional expression from a *GAL1* promoter is used to measure Far1 half-life ± SE pre-*Start* as in (C), but for a range of pheromone concentrations. Error bars in (D) and (G) denote SEM.

demonstrate the requirement of Far1 stability pre- and post-*Start* for intra- and inter-generational memory respectively.

Far1 Stability during Arrest Peaks at Intermediate Pheromone Concentrations

The clear connection between Far1-based memory and protein stability suggested the possibility that WT cells might modulate Far1 stability to regulate memory. To test this possibility, we measured *FAR1* half-life by expressing it from the *GAL1* promoter and shutting off transcription (Figure 6C). However, we now measure the half-life during pre-*Start* for cells growing in 0, 3, 6, or 240 nM pheromone. We found that Far1 stability peaked at 3 nM with a ~150 min half-life (Figures 6G and S7H and S7I). Far1 stability was reduced to ~100 min in

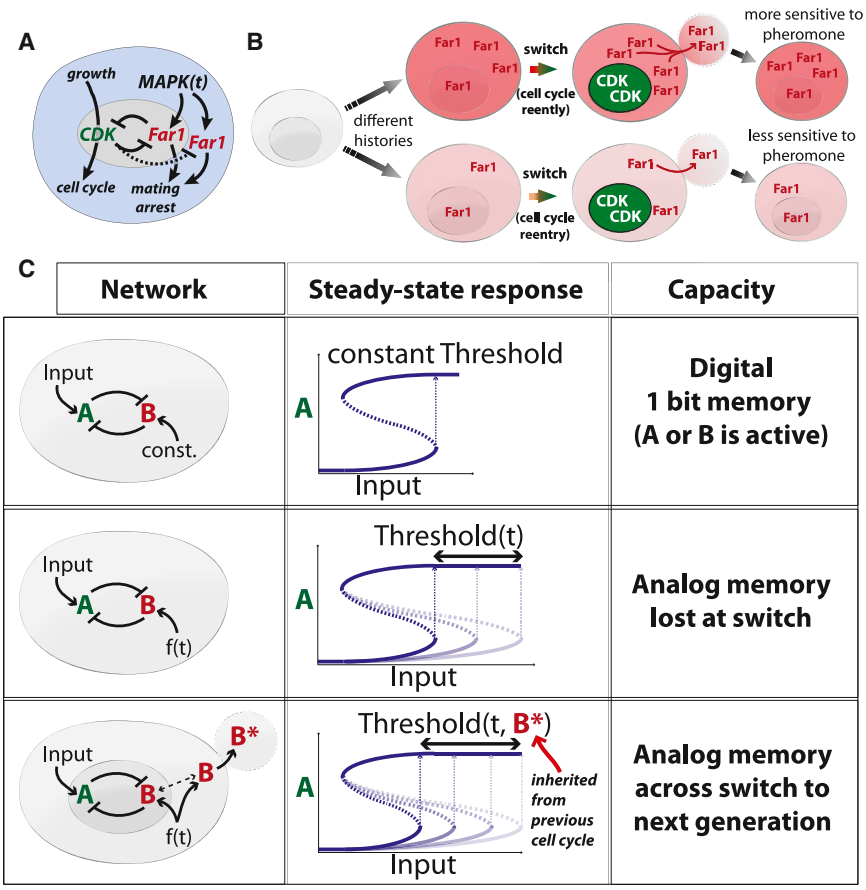

Figure 7. Compartmentalization Enables Analog Memory to Pass through a Bistable Switch

(A) The *Start* regulatory network regulating the proliferation-differentiation decision in budding yeast is a bistable switch.

(B) Inheritance of cytoplasmic Far1 forms the mechanistic basis of intergenerational memory of pheromone exposure.

(C) Top: a double-negative switch with constant signal activating B results in a bistable switch with a single bit of memory, i.e., did the input approach its current level from above or below. Middle: a time-dependent f(t) signal activates B to allow the time-dependent threshold to encode an analog memory of f(t). However, this memory is lost by inactivation upon triggering the double-negative switch. Bottom: compartmentalization allows transmission of analog memory of the time-dependent f(t) signal across the double-negative (positive) feedback switch.

0 and 240 nM pheromone. We speculate that this decreased stability might arise from increased G1 cyclin and Fus3 MAPK kinase activities. It is interesting to note that the maximum half-life, i.e., maximal memory, occurs right where the decision to reenter the cell cycle is most sensitive to pheromone concentration.

DISCUSSION

To inform our decisions, our experiences are sensed, encoded, and stored as memories. Like us, individual cells also rely on past experience to inform their most important decisions. In budding yeast, one of the most important decisions is whether or not to proliferate or to arrest division and attempt to mate with another haploid cell. Budding yeast invest heavily in this decision, as mutations eliminating the ability to mate provide a ~2% growth rate advantage in pheromone-free conditions (Lang et al., 2009). Perhaps not surprisingly, several distinct types of memory regulate this proliferation-differentiation decision.

The simplest type of memory informing yeast mating is binary and stored as a single bit of information. For example, due to its asymmetric division pattern, a budding yeast cell is either a mother or a daughter. With regards to mating, this bit matters because mother cells are less sensitive to pheromone than daughter cells (Moore, 1984). In part, this is likely due to the differential expression of *CLN3,* the upstream cyclin driving cell-cycle progression in G1 (Laabs et al., 2003). Mother cells produce a burst of *CLN3* expression at the transition from mitosis to G1, while daughter cells do not due to the daughter-specific transcription factors, Ace2 and Ash1 (Di Talia et al., 2009). In addition, differential post-transcriptional regulation of *CLN3* in mother and daughter cells may be due to Whi3 (Caudron and Barral, 2013), which both decreases *CLN3* message stability and translation rate (Cai and Futcher, 2013; Garí et al., 2001; Holmes et al., 2013). Yet, all this information pertaining being a mother or daughter cell is binary.

Previously, we identified a continuous, analog form of memory of past pheromone exposure that informs the decision to reenter the cell cycle from pheromone arrest (Doncic and Skotheim, 2013). Cells experiencing higher pheromone concentrations over longer periods of time are more reluctant to reenter the cell cycle. While MAPK pathway activity rapidly responds to reflect the current extracellular pheromone concentration, proteins are more stable so that their level will reflect an integral of past pathway activity (Colman-Lerner et al., 2005; Takahashi and Pryciak, 2008; Yu et al., 2008). More specifically, Far1 accumulates at a monotonically increasing rate with pheromone concentration so that its total amount reflects a combination of arrest duration and pheromone concentration (Chang and Herskowitz, 1990; Doncic and Skotheim, 2013). Thus, the amount of Far1 accumulated during pheromone arrest reflects an integral of pathway activity over time that encodes the history of pheromone exposure into a continuous analog rather than binary variable. However, the mutual inhibition of Far1 and Cdk activities suggested that this analog memory, i.e., the accumulated Far1, would be lost upon flipping the cell-cycle switch (Figures 7A–7C).

Here, we show how the distribution of Far1 into nuclear and cytoplasmic compartments is used to transmit the analog memory of pheromone exposure across the cell cycle switch to the next generation. While nuclear Far1 is rapidly degraded, as expected by the double-negative switch, cytoplasmic Far1 is longer lived and continually synthesized so that a significant amount remains at the end of the cell cycle to be inherited by daughter cells. We show here that this inherited Far1 contributes to increased pheromone sensitivity and thereby allows mother cells to transmit intergenerational memory of pheromone exposure to their daughter cells. We also identified a fraction of fixed cytoplasmic Far1 as key to storing intergenerational memory. If some Far1 were not fixed in the cytoplasm, it would likely be rapidly degraded post-*Start* due to the high nuclear B-type cyclin activity. While this Far1 fraction is fixed on the minute timescale, we suspect that it is not permanently fixed because nuclear Far1 is important for maintaining the cell-cycle arrest to which the inherited cytoplasmic Far1 eventually contributes. Thus, the slow dissociation of the fixed Far1 is likely central to reading the intergenerational memory of pheromone exposure.

Protein stability is central to both intra- and intergenerational Far1-based analog memory as destabilizing mutations eliminate both. In general, protein stability determines the timescale on which the cell can remember past events. For rapidly degraded proteins, levels will simply reflect the current state of the cell, while for stable proteins, levels will reflect their synthesis over longer periods of time so that their amount can be used to store long-term memories on the timescale of dilution due to cell growth. The demonstrated ability of the cell to regulate protein stability over a wide range of temporal and spatial scales suggests that the analog memory mechanisms discussed here can be easily tuned through mutation and selection.

More broadly, our work illustrates how spatial organization can greatly expand the functionality of signaling motifs. Recently, it has been shown how positive feedback can be enhanced by protein transport within the mammalian mitotic switch (Santos et al., 2012). Activation of Cdk1-Cyclin B complexes within the nucleus recruit additional such complexes to dramatically ramp up nuclear Cdk activity without protein synthesis. However, this represents an enhancement of the well-known ability of positive feedback circuits to generate sharp switches. Here, we have shown how spatial organization allows memory to be transmitted across a positive feedback-driven switch to enable an entirely new and unexpected property of this well-characterized signaling motif. Given the extensive spatial organization within cells, we expect this example to be the first of many in which new signal-processing properties of network motifs are enabled by compartmentalization.

EXPERIMENTAL PROCEDURES

See additional Supplemental Information for methods regarding confocal microscopy, FRAP, western blot and kinase assays shown in Figures 2 and 3.

Wide-Field Time Lapse Microscopy and Analysis

A Zeiss Observer Z1 microscope with an automated stage using a plan-apo 63X/1.4NA oil immersion objective and Definite Focus hardware was used to take images every 3 min (6 min for the *FAR1-L92P* strains). We used a Cellasic microfluidics device (http://www.cellasic.com/) with Y04C plates. *WHI5-mCherry, FAR1-Venus* and *FAR1-GFP* strains were exposed for 750 ms, 300 ms or 150–300 ms using the Colibri 540-80, 505 or 470 LED modules respectively at 25% power. There was no significant photobleaching at our sampling rate (Figure S7J). *FAR1* activity is not affected by fusion to a fluorescent protein (Doncic and Skotheim, 2013). Image segmentation and quantification was performed as described in (Doncic et al., 2013). We often plot mean values and their associated SE because this gives a graphical representation of statistical significance. Corresponding full distributions can be found in the Supplemental Information.

Measurement of Inherited Far1

For each cell we determine inherited Far1 to be (Far1-Venus signal – baseline)/(baseline). "Normalized inherited Far1" is the amount at the beginning of G1 above what that cell would be expected to have when cycling in pheromone-free media (see also schematic S2I and Supplemental Information for details).

Strains and Media

All strains are congenic with W303 (see Table S1) and were constructed using standard methods. Yeast were grown in synthetic complete media with 2% glucose unless otherwise stated (2% galactose were used for the Far1 stability experiments in Figures 3 and 6). Before an experiment, cells were grown to an OD < 0.1 after which they were sonicated for ~5 s at 3W intensity. All media were mixed with 20 mg/ml casein (Sigma) to inhibit α-factor surface adhesion (Colman-Lerner et al., 2005).

SUPPLEMENTAL INFORMATION

Supplemental Information includes Extended Experimental Procedures, seven figures, and two tables and can be found with this article online at http://dx.doi.org/10.1016/j.cell.2015.02.032.

AUTHOR CONTRIBUTIONS

A.D. and J.M.S. designed the study. A.D. and O.A. performed all experiments with the following exceptions. E.V. and M.L. identified of the *FAR1-L92P* mutant and performed the Fus3 activity measurements (Figures 3I–3L). A.G., A.B., G.V., and A.C.-L. performed the FRAP experiments (Figure 2). A.D., O.A., and J.M.S. wrote the paper.

ACKNOWLEDGMENTS

Research in the Skotheim laboratory was supported by the Burroughs Wellcome Fund (CASI) and the NIH (GM092925). The Colman-Lerner laboratory was supported by grant PICT2010-2248 from the Argentine Agency of Research and Technology (ANPCyT) and the NIH (GM097479), while the Loog laboratory was supported by Estonian Science Agency Grant IUT2-21.

Received: July 27, 2014
Revised: November 24, 2014
Accepted: January 17, 2015
Published: March 12, 2015

REFERENCES

Alon, U. (2007). Network motifs: theory and experimental approaches. Nat. Rev. Genet. *8*, 450–461.

Behar, M., Hao, N., Dohlman, H.G., and Elston, T.C. (2008). Dose-to-duration encoding and signaling beyond saturation in intracellular signaling networks. PLoS Comput. Biol. *4*, e1000197.

Blackwell, E., Halatek, I.M., Kim, H.J., Ellicott, A.T., Obukhov, A.A., and Stone, D.E. (2003). Effect of the pheromone-responsive G(alpha) and phosphatase proteins of Saccharomyces cerevisiae on the subcellular localization of the Fus3 mitogen-activated protein kinase. Mol. Cell. Biol. *23*, 1135–1150.

Blondel, M., Alepuz, P.M., Huang, L.S., Shaham, S., Ammerer, G., and Peter, M. (1999). Nuclear export of Far1p in response to pheromones requires the export receptor Msn5p/Ste21p. Genes Dev. *13*, 2284–2300.

Blondel, M., Galan, J.M., Chi, Y., Lafourcade, C., Longaretti, C., Deshaies, R.J., and Peter, M. (2000). Nuclear-specific degradation of Far1 is controlled by the localization of the F-box protein Cdc4. EMBO J. *19*, 6085–6097.

Cai, Y., and Futcher, B. (2013). Effects of the yeast RNA-binding protein Whi3 on the half-life and abundance of CLN3 mRNA and other targets. PLoS ONE *8*, e84630.

Caudron, F., and Barral, Y. (2013). A super-assembly of Whi3 encodes memory of deceptive encounters by single cells during yeast courtship. Cell *155*, 1244–1257.

Chang, F., and Herskowitz, I. (1990). Identification of a gene necessary for cell cycle arrest by a negative growth factor of yeast: FAR1 is an inhibitor of a G1 cyclin, CLN2. Cell *63*, 999–1011.

Chen, R.E., and Thorner, J. (2007). Function and regulation in MAPK signaling pathways: lessons learned from the yeast Saccharomyces cerevisiae. Biochim. Biophys. Acta *1773*, 1311–1340.

Colman-Lerner, A., Gordon, A., Serra, E., Chin, T., Resnekov, O., Endy, D., Pesce, C.G., and Brent, R. (2005). Regulated cell-to-cell variation in a cell-fate decision system. Nature *437*, 699–706.

Costanzo, M., Nishikawa, J.L., Tang, X., Millman, J.S., Schub, O., Breitkreuz, K., Dewar, D., Rupes, I., Andrews, B., and Tyers, M. (2004). CDK activity antagonizes Whi5, an inhibitor of G1/S transcription in yeast. Cell *117*, 899–913.

de Bruin, R.A., McDonald, W.H., Kalashnikova, T.I., Yates, J., 3rd, and Wittenberg, C. (2004). Cln3 activates G1-specific transcription via phosphorylation of the SBF bound repressor Whi5. Cell *117*, 887–898.

Di Talia, S., Wang, H., Skotheim, J.M., Rosebrock, A.P., Futcher, B., and Cross, F.R. (2009). Daughter-specific transcription factors regulate cell size control in budding yeast. PLoS Biol. *7*, e1000221.

Doncic, A., and Skotheim, J.M. (2013). Feedforward regulation ensures stability and rapid reversibility of a cellular state. Mol. Cell *50*, 856–868.

Doncic, A., Falleur-Fettig, M., and Skotheim, J.M. (2011). Distinct interactions select and maintain a specific cell fate. Mol. Cell *43*, 528–539.

Doncic, A., Eser, U., Atay, O., and Skotheim, J.M. (2013). An algorithm to automate yeast segmentation and tracking. PLoS ONE *8*, e57970.

Errede, B., and Ammerer, G. (1989). STE12, a protein involved in cell-type-specific transcription and signal transduction in yeast, is part of protein-DNA complexes. Genes Dev. *3*, 1349–1361.

Evangelista, M., Blundell, K., Longtine, M.S., Chow, C.J., Adames, N., Pringle, J.R., Peter, M., and Boone, C. (1997). Bni1p, a yeast formin linking cdc42p and the actin cytoskeleton during polarized morphogenesis. Science *276*, 118–122.

Forney, G.D. (1973). Viterbi Algorithm. IEEE *61*, 268–278.

Garí, E., Volpe, T., Wang, H., Gallego, C., Futcher, B., and Aldea, M. (2001). Whi3 binds the mRNA of the G1 cyclin CLN3 to modulate cell fate in budding yeast. Genes Dev. *15*, 2803–2808.

Garrenton, L.S., Braunwarth, A., Irniger, S., Hurt, E., Künzler, M., and Thorner, J. (2009). Nucleus-specific and cell cycle-regulated degradation of mitogen-activated protein kinase scaffold protein Ste5 contributes to the control of signaling competence. Mol. Cell. Biol. *29*, 582–601.

Gartner, A., Jovanović, A., Jeoung, D.I., Bourlat, S., Cross, F.R., and Ammerer, G. (1998). Pheromone-dependent G1 cell cycle arrest requires Far1 phosphorylation, but may not involve inhibition of Cdc28-Cln2 kinase, in vivo. Mol. Cell. Biol. *18*, 3681–3691.

Hao, N., Nayak, S., Behar, M., Shanks, R.H., Nagiec, M.J., Errede, B., Hasty, J., Elston, T.C., and Dohlman, H.G. (2008). Regulation of cell signaling dynamics by the protein kinase-scaffold Ste5. Mol. Cell *30*, 649–656.

Hartwell, L.H., Culotti, J., Pringle, J.R., and Reid, B.J. (1974). Genetic control of the cell division cycle in yeast. Science *183*, 46–51.

Henchoz, S., Chi, Y., Catarin, B., Herskowitz, I., Deshaies, R.J., and Peter, M. (1997). Phosphorylation- and ubiquitin-dependent degradation of the cyclin-dependent kinase inhibitor Far1p in budding yeast. Genes Dev. *11*, 3046–3060.

Holmes, K.J., Klass, D.M., Guiney, E.L., and Cyert, M.S. (2013). Whi3, an S. cerevisiae RNA-binding protein, is a component of stress granules that regulates levels of its target mRNAs. PLoS ONE *8*, e84060.

Howell, A.S., Jin, M., Wu, C.F., Zyla, T.R., Elston, T.C., and Lew, D.J. (2012). Negative feedback enhances robustness in the yeast polarity establishment circuit. Cell *149*, 322–333.

Jeoung, D.I., Oehlen, L.J., and Cross, F.R. (1998). Cln3-associated kinase activity in Saccharomyces cerevisiae is regulated by the mating factor pathway. Mol. Cell. Biol. *18*, 433–441.

Kholodenko, B.N., Hancock, J.F., and Kolch, W. (2010). Signalling ballet in space and time. Nat. Rev. Mol. Cell Biol. *11*, 414–426.

Laabs, T.L., Markwardt, D.D., Slattery, M.G., Newcomb, L.L., Stillman, D.J., and Heideman, W. (2003). ACE2 is required for daughter cell-specific G1 delay in Saccharomyces cerevisiae. Proc. Natl. Acad. Sci. USA *100*, 10275–10280.

Lang, G.I., Murray, A.W., and Botstein, D. (2009). The cost of gene expression underlies a fitness trade-off in yeast. Proc. Natl. Acad. Sci. USA *106*, 5755–5760.

Lanker, S., Valdivieso, M.H., and Wittenberg, C. (1996). Rapid degradation of the G1 cyclin Cln2 induced by CDK-dependent phosphorylation. Science *271*, 1597–1601.

Lee, M.J., Ye, A.S., Gardino, A.K., Heijink, A.M., Sorger, P.K., MacBeath, G., and Yaffe, M.B. (2012). Sequential application of anticancer drugs enhances cell death by rewiring apoptotic signaling networks. Cell *149*, 780–794.

Malleshaiah, M.K., Shahrezaei, V., Swain, P.S., and Michnick, S.W. (2010). The scaffold protein Ste5 directly controls a switch-like mating decision in yeast. Nature *465*, 101–105.

McKinney, J.D., Chang, F., Heintz, N., and Cross, F.R. (1993). Negative regulation of FAR1 at the Start of the yeast cell cycle. Genes Dev. *7*, 833–843.

Moore, S.A. (1984). Yeast cells recover from mating pheromone alpha factor-induced division arrest by desensitization in the absence of alpha factor destruction. J. Biol. Chem. *259*, 1004–1010.

Nagiec, M.J., and Dohlman, H.G. (2012). Checkpoints in a yeast differentiation pathway coordinate signaling during hyperosmotic stress. PLoS Genet. *8*, e1002437.

Nern, A., and Arkowitz, R.A. (1999). A Cdc24p-Far1p-Gbetagamma protein complex required for yeast orientation during mating. J. Cell Biol. *144*, 1187–1202.

Nern, A., and Arkowitz, R.A. (2000). Nucleocytoplasmic shuttling of the Cdc42p exchange factor Cdc24p. J. Cell Biol. *148*, 1115–1122.

Oehlen, L.J., McKinney, J.D., and Cross, F.R. (1996). Ste12 and Mcm1 regulate cell cycle-dependent transcription of FAR1. Mol. Cell. Biol. *16*, 2830–2837.

Oehlen, L.J., Jeoung, D.I., and Cross, F.R. (1998). Cyclin-specific START events and the G1-phase specificity of arrest by mating factor in budding yeast. Mol. Gen. Genet. *258*, 183–198.

Peter, M., and Herskowitz, I. (1994). Direct inhibition of the yeast cyclin-dependent kinase Cdc28-Cln by Far1. Science *265*, 1228–1231.

Peter, M., Gartner, A., Horecka, J., Ammerer, G., and Herskowitz, I. (1993). FAR1 links the signal transduction pathway to the cell cycle machinery in yeast. Cell *73*, 747–760.

Pope, P.A., Bhaduri, S., and Pryciak, P.M. (2014). Regulation of Cyclin-Substrate Docking by a G1 Arrest Signaling Pathway and the Cdk Inhibitor Far1. Curr. Biol.

Pryciak, P.M., and Huntress, F.A. (1998). Membrane recruitment of the kinase cascade scaffold protein Ste5 by the Gbetagamma complex underlies activation of the yeast pheromone response pathway. Genes Dev. *12*, 2684–2697.

Purvis, J.E., Karhohs, K.W., Mock, C., Batchelor, E., Loewer, A., and Lahav, G. (2012). p53 dynamics control cell fate. Science *336*, 1440–1444.

Qi, M., and Elion, E.A. (2005). Formin-induced actin cables are required for polarized recruitment of the Ste5 scaffold and high level activation of MAPK Fus3. J. Cell Sci. *118*, 2837–2848.

Raj, A., van den Bogaard, P., Rifkin, S.A., van Oudenaarden, A., and Tyagi, S. (2008). Imaging individual mRNA molecules using multiple singly labeled probes. Nat. Methods *5*, 877–879.

Santos, S.D., Wollman, R., Meyer, T., and Ferrell, J.E., Jr. (2012). Spatial positive feedback at the onset of mitosis. Cell *149*, 1500–1513.

Shimada, Y., Gulli, M.P., and Peter, M. (2000). Nuclear sequestration of the exchange factor Cdc24 by Far1 regulates cell polarity during yeast mating. Nat. Cell Biol. *2*, 117–124.

Shirayama, M., Tóth, A., Gálová, M., and Nasmyth, K. (1999). APC(Cdc20) promotes exit from mitosis by destroying the anaphase inhibitor Pds1 and cyclin Clb5. Nature *402*, 203–207.

Skotheim, J.M., Di Talia, S., Siggia, E.D., and Cross, F.R. (2008). Positive feedback of G1 cyclins ensures coherent cell cycle entry. Nature *454*, 291–296.

Strickfaden, S.C., Winters, M.J., Ben-Ari, G., Lamson, R.E., Tyers, M., and Pryciak, P.M. (2007). A mechanism for cell-cycle regulation of MAP kinase signaling in a yeast differentiation pathway. Cell *128*, 519–531.

Takahashi, S., and Pryciak, P.M. (2008). Membrane localization of scaffold proteins promotes graded signaling in the yeast MAP kinase cascade. Curr. Biol. *18*, 1184–1191.

Thomson, T.M., Benjamin, K.R., Bush, A., Love, T., Pincus, D., Resnekov, O., Yu, R.C., Gordon, A., Colman-Lerner, A., Endy, D., and Brent, R. (2011). Scaffold number in yeast signaling system sets tradeoff between system output and dynamic range. Proc. Natl. Acad. Sci. USA *108*, 20265–20270.

Torres, M.P., Clement, S.T., Cappell, S.D., and Dohlman, H.G. (2011). Cell cycle-dependent phosphorylation and ubiquitination of a G protein alpha subunit. J. Biol. Chem. *286*, 20208–20216.

Tyers, M., and Futcher, B. (1993). Far1 and Fus3 link the mating pheromone signal transduction pathway to three G1-phase Cdc28 kinase complexes. Mol. Cell. Biol. *13*, 5659–5669.

Valtz, N., Peter, M., and Herskowitz, I. (1995). FAR1 is required for oriented polarization of yeast cells in response to mating pheromones. J. Cell Biol. *131*, 863–873.

Yang, Q., and Ferrell, J.E., Jr. (2013). The Cdk1-APC/C cell cycle oscillator circuit functions as a time-delayed, ultrasensitive switch. Nat. Cell Biol. *15*, 519–525.

Yosef, N., and Regev, A. (2011). Impulse control: temporal dynamics in gene transcription. Cell *144*, 886–896.

Yu, R.C., Pesce, C.G., Colman-Lerner, A., Lok, L., Pincus, D., Serra, E., Holl, M., Benjamin, K., Gordon, A., and Brent, R. (2008). Negative feedback that improves information transmission in yeast signalling. Nature *456*, 755–761.